

# Structural basis for selectivity of the isoquinoline sulfonamide family of protein kinase inhibitors

[casein kinase-1/*N*-(2-aminoethyl)-5-chloroisoquinoline-8-sulfonamide/isoquinoline ring-flipping/x-ray crystallography/molecular modelling]

RUI-MING XU\*, GILLES CARMEL\*†, JEFF KURET‡, AND XIAODONG CHENG\*§

\*W.M. Keck Structural Biology Laboratory, Cold Spring Harbor Laboratory, Cold Spring Harbor, NY 11724; and †Department of Cell and Molecular Biology, Northwestern University Medical School, Chicago, IL 60611

Communicated by Michael Wigler, Cold Spring Harbor Laboratory, Cold Spring Harbor, NY, February 22, 1996 (received for review October 17, 1995)

**ABSTRACT** A large family of isoquinoline sulfonamide compounds inhibits protein kinases by competing with adenosine triphosphates (ATP), yet interferes little with the activity of other ATP-using enzymes such as ATPases and adenylate cyclases. One such compound, *N*-(2-aminoethyl)-5-chloroisoquinoline-8-sulfonamide (CKI7), is selective for casein kinase-1 isolated from a variety of sources. Here we report the crystal structure of the catalytic domain of *Schizosaccharomyces pombe* casein kinase-1 complexed with CKI7, refined to a crystallographic R-factor of 17.8% at 2.5 Å resolution. The structure provides new insights into the mechanism of the ATP-competing inhibition and the origin of their selectivity toward different protein kinases. Selectivity for protein kinases versus other enzymes is achieved by hydrophobic contacts and the hydrogen bond with isoquinoline ring. We propose that the hydrogen bond involving the ring nitrogen-2 atom of the isoquinoline must be preserved, but that the ring can flip depending on the chemical substituents at ring positions 5 and 8. Selectivity for individual members of the protein kinase family is achieved primarily by interactions with these substituents.

Casein kinase-1 (CK1) is an ubiquitous eukaryotic protein kinase that phosphorylates acidic substrate recognition sequences (1, 2). Functionally, CK1 is known to phosphorylate a number of proteins *in vitro* including SV40 T-antigen (3) and tumor suppressor p53 (4). CK1 is also known to participate in the DNA repair pathways in lower eukaryotes (5). Structurally, CK1 folds, like other protein kinases, into two lobes: a small N-terminal lobe that contains predominantly  $\beta$ -sheets and a large, mostly  $\alpha$ -helical, C-terminal lobe (6). The two lobes are connected by a single loop formed by a conserved decapeptide segment (amino acids 86–95) in the CK1 family. Adenosine triphosphate (ATP) binds in the cleft formed between the two lobes.

By including chemical substituents at two positions of the isoquinoline ring (positions 5 and 8; Table 1), inhibitors selective for different protein kinases have been obtained (11, 12). Thus, individual isoquinoline sulfonamides have emerged as important pharmacological tools for dissecting signal transduction pathways. *N*-(2-aminoethyl)-5-chloroisoquinoline-8-sulfonamide (CKI7), which has a chlorine at ring position 5 and an ethylamine sulfonamide at ring position 8 (ref. 7; Table 1), inhibits mammalian and *Schizosaccharomyces pombe* CK1 with a  $K_i$  of 8.5  $\mu$ M (7) and 39  $\mu$ M (10), respectively. We now report on the crystal structure of a binary complex between CKI7 and yeast catalytic domain of CK1.

The publication costs of this article were defrayed in part by page charge payment. This article must therefore be hereby marked "advertisement" in accordance with 18 U.S.C. §1734 solely to indicate this fact.

## MATERIALS AND METHODS

**Crystallization and Data Collection.** The recombinant 298-residue catalytic core of Cki1, one of four CK1 isoforms in fission yeast (10), was expressed and purified as described (13). CKI7 was obtained from Seikagaku America (Rockville, MD). The CK1–CKI7 complex was formed by mixing the protein (10 mg/ml in 10 mM Mops, pH 7.0/50 mM NaCl/0.1 mM EGTA/0.1% 2-mercaptoethanol/1 mM DTT) and CKI7 (2 mM in 2% dimethyl sulfoxide; diluted from a 100-mM solution in dimethyl sulfoxide) at room temperature. The complex was crystallized by the hanging drop method at 16°C against a well solution of 2% methanol, 1.4–1.7 M ammonium sulfate, and 2.5–25 mM sodium acetate at pH 4.6. Hexagonal crystals ( $a = b = 98$  Å,  $c = 219$  Å) of considerable size ( $>0.5$  mm) appeared in all conditions, but they only diffracted to 3.5-Å resolution. Smaller ( $\sim 0.1$  mm) trigonal crystals (space group  $P3_221$ ,  $a = b = 79.10$  Å,  $c = 120.04$  Å) also appeared in drops with 2.5–5 mM sodium acetate. These smaller trigonal crystals diffracted x-rays to higher than 2.5 Å resolution at beam line X12-C of the National Synchrotron Light Source (Brookhaven National Laboratory). Diffraction data from a single crystal were collected at room temperature with an MAR image plate detector, and processed using the HKL software package (ref. 14; Table 2).

**Structure Determination and Refinement.** The structure of the inhibitory complex was determined by difference Fourier synthesis using the CK1 coordinates from the CK1–MgATP structure (6). The atomic coordinates of CK1 were refined against the diffraction data using X-PLOR (15). Initially, a 120-cycle positional refinement followed by simulated annealing from a temperature of 3000 K to 300 K brought the crystallographic R-factor from 34% to 25% using data in the resolution range of 8.0–2.5 Å. At this stage, the difference map ( $F_o - F_c$ ,  $\alpha_c$ ) clearly showed the CKI7 electron density. Subsequent refinement used all measured data from 31.0 to 2.5 Å. Ten rounds of positional and individual temperature refinements of the protein model were carried out without CKI7. Each round of refinement was followed by manual refitting and placement of well-ordered solvent molecules using the graphics program O (16), and then, bulk solvent correction using X-PLOR. The solvent scattering density and isotropic temperature factor for the solvent component were determined by

Abbreviations: CKI7, *N*-(2-aminoethyl)-5-chloroisoquinoline-8-sulfonamide; CKI6, *N*-(2-aminoethyl)-8-isoquinolinesulfonamide; H9, *N*-(2-aminoethyl)-5-isoquinolinesulfonamide; CK1, casein kinase-1; cAPK, cyclic AMP-dependent protein kinase; ATP, adenosine triphosphate.

Data deposition: The atomic coordinates and structure factors have been deposited in the Protein Data Bank, Chemistry Department, Brookhaven National Laboratory, Upton, NY 11973 (reference 2csn).

†Present address: Genome Therapeutics Corporation, 100 Beaver Street, Waltham, MA 02154.

§To whom reprint requests should be addressed.

Table 1. Chemical structure of CKI7 and different substitutions at positions 5 and 8

Inhibitor	Ring position 5	Ring position 8	$K_i$ , $\mu\text{M}^*$	
			CK1 <sup>†</sup>	cAPK <sup>‡</sup>
CKI7	Cl	$-\text{SO}_2\text{NH}(\text{CH}_2)_2\text{NH}_2$	8.5	550
CKI6	H	$-\text{SO}_2\text{NH}(\text{CH}_2)_2\text{NH}_2$	50	>1000
H9	$-\text{SO}_2\text{NH}(\text{CH}_2)_2\text{NH}_2$	H	110	3.6
H89	$-\text{SO}_2\text{NH}(\text{CH}_2)_2\text{NHCH}_2\text{CH}=\text{CH}-\text{C}_6\text{H}_4-\text{Br}$	H	38	0.05

\*This table is a summary of refs. 7–9.

<sup>†</sup>Mammalian CK1 from bovine testis. The  $K_i$  of CKI7 for fission yeast CK1 is 39  $\mu\text{M}$  (10).

<sup>‡</sup>Mammalian cAPK from bovine heart.

minimizing the crystallographical R-factor using diffraction data in the lowest resolution range of 31.0–6.0 Å (1100 reflections). An additional 10 rounds of refinements were performed with the CKI7 model included. The initial CKI7 molecule was generated using modelling program MACROMODEL (17), and manually fit into the density. The final CK1–CKI7 atomic model included 157 ordered water molecules and 2 sulfate ions.

**Molecular Modelling.** The *N*-(2-aminoethyl)-5-isoquinolinesulfonamide (H9) molecule was modelled using molecular modelling program MACROMODEL version 4.5 (17). A Monte Carlo conformational search was first performed with 5000 internally generated trial structures. Conjugate gradient energy minimization in the absence of solvent was carried out during the course of the conformational search, using the MM2 force field of MACROMODEL. A total of 449 conformations were found with an energy within 10 kcal/mol from the global minimum. These conformers were subjected to further energy minimization in the presence of water and resulted in

188 unique conformations within 10 kcal/mol of the global minimum, among which 56 conformations were within 1.0 kcal/mol. These 56 structures were examined using graphics program O (16) for best fit with cyclic AMP-dependent protein kinase (cAPK) structure by visual inspection. The H9 molecule shown here represents the best fit from these 56 candidates.

## RESULTS AND DISCUSSION

**CK1–CKI7 Overall Structure.** In the CK1–CKI7 structure, the overall folding of CK1 and the spatial positions of its ordered sidechains closely resemble those found in the CK1–MgATP complex described in ref. 6. The root-mean-square deviation is 0.39 Å when the C $\alpha$  atoms of the two structures are least-squares aligned. In this superposition, CKI7 is found to occupy the same cleft that binds ATP. The isoquinoline ring replaces the adenine ring, whereas the ethylamine sulfonamide chain of CKI7 points away from the triphosphate moiety of ATP (Fig. 14). Thus, it is structurally confirmed that CKI7,

Table 2. Crystallographic data and refinement

Resolution range, Å	Crystals	Total measured reflections	Unique reflections	I/ $\sigma$	$R_{\text{merge}}$ ,* %
$\infty - 2.3$	1	94,790	18,581	$\geq 0$	6.9
			16,391	$\geq 2$	6.2
Resolution shell, Å	Completeness, % (I/ $\sigma \geq 2$ )		R-factor <sup>†</sup> , %		
31.0–4.99	92.3		20.9		
4.99–3.97	94.9		13.7		
3.97–3.47	94.2		14.5		
3.47–3.15	92.4		16.7		
3.15–2.92	88.9		18.4		
2.92–2.75	86.6		21.4		
2.75–2.61	80.2		22.0		
2.61–2.50	69.0		23.6		
31.0–2.50	87.4		17.8		
Root-mean-square deviation from ideality					
Nonhydrogen atoms		Bond lengths, Å	Bond angles, °		
CK1	2386	0.012	1.63		
CKI7	18				
Water	157				
Sulfate	10				

\* $R_{\text{merge}} = 100 \times \sum |I - \langle I \rangle| / \sum \langle I \rangle$ , where  $I$  is the measured intensity of each reflection and  $\langle I \rangle$  is the intensity averaged from multiple observations of symmetry related reflections.

<sup>†</sup>R-factor =  $100 \times \sum |F_O - F_C| / \sum |F_O|$ , where  $F_O$  and  $F_C$  are the observed and calculated structure factor amplitudes, respectively.

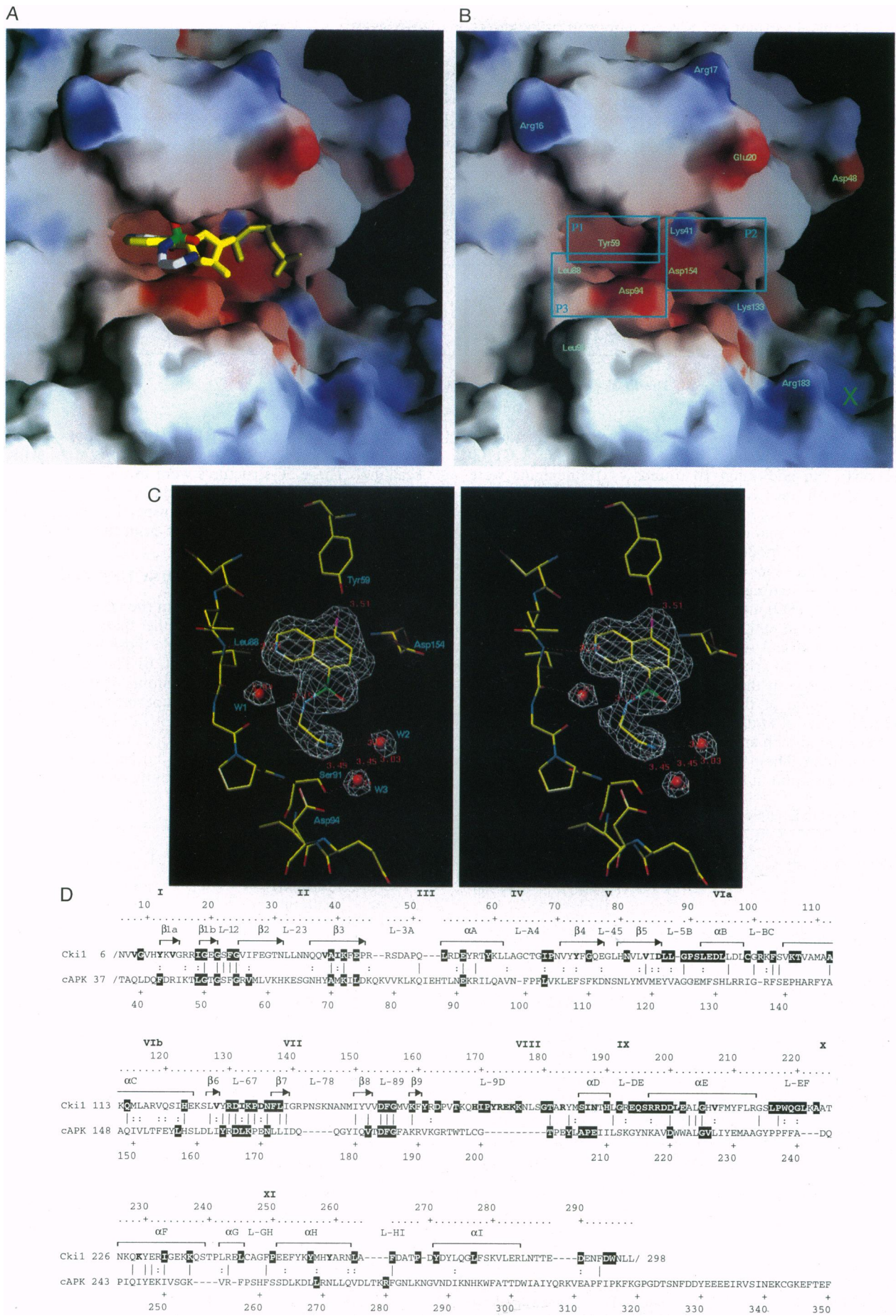


FIG. 1. (Legend appears at the bottom of the opposite page.)



and presumably the entire family of isoquinoline sulfonamide inhibitors, bind their respective protein kinases stoichiometrically by competing with ATP for its binding cleft (8).

Despite these similarities, two major differences in CK1 conformation are apparent in the CK1–CKI7 and CK1–MgATP complexes. First, the sidechain of Asp<sup>154</sup> of loop L-89 (Fig. 1D), which hydrogen bonds with Asn<sup>136</sup> in the CK1–MgATP structure, adopts a different conformation forming a salt bridge with Lys<sup>41</sup>. In the CK1–MgATP structure, Lys<sup>41</sup> interacts with  $\alpha$  and  $\beta$  phosphates of ATP and Asn<sup>136</sup> coordinates with Mg<sup>2+</sup>. Lys<sup>41</sup> and Asp<sup>154</sup> are two of the five invariant amino acids found in protein kinases and Asn<sup>136</sup> is conserved in all serine/threonine kinases (19, 20). Second, the tip of the glycine-rich  $\beta$ 1-turn- $\beta$ 2 motif (Ser<sup>22</sup>-Phe-Gly<sup>24</sup>; loop L-12), which interacts with the triphosphate moiety of ATP in the CK1–MgATP structure, is tilted toward the cleft in the CK1–CKI7 structure.

**Nucleotide-Binding Cleft: P1, P2, and P3 Sites.** The nucleotide-binding cleft can be described as consisting of three structurally distinctive sites designated P1, P2, and P3 (Fig. 1B). The hydrophobic P1 site hosts both the adenine ring of ATP and the isoquinoline ring of CKI7, whereas the solvent-accessible P2 site, comprised by many of the charged invariant amino acids found in all protein kinases, binds the triphosphate moiety of ATP. A third area, P3, where the ethylamine sulfonamide chain of CKI7 binds, is also solvent accessible and consists of sequences that vary greatly among protein kinases.

**Hydrogen Bonding at P1 Site.** Closer inspection reveals that the N2 atom of the isoquinoline ring, the only nitrogen on the isoquinoline ring, lies in a position that is occupied by the N1 atom of the adenine ring of ATP in the CK1–ATP complex. Both of these nitrogen atoms form hydrogen bonds with the backbone amide of Leu<sup>88</sup> in their respective complexes (Fig. 2A and B), suggesting that this interaction makes an important contribution to the binding affinity of CKI7. Crystallographic studies of several eukaryotic protein kinases have shown commonality in the interaction between the N1 of ATP and the mainchain nitrogen atoms, e.g., the mainchain nitrogens of Val<sup>123</sup> in the cAPK (21; see Fig. 1D), Leu<sup>83</sup> in cyclin-dependent kinase 2 (22), Met<sup>106</sup> of the MAP kinase ERK2 (23), and Met<sup>106</sup> of glycogen phosphorylase kinase (24), suggesting that this hydrogen bond between protein kinases and ATP (and potentially isoquinoline sulfonamides) is probably conserved in most protein kinases. Indeed, Hidaka *et al.* (25) noted that naphthalene sulfonamides were not selective protein kinase inhibitors until the ring from the all-carbon naphthalene was changed to the nitrogen-containing isoquinoline. Moreover, comparison of the interactions among cyclin-dependent kinase 2 with ATP and cyclin-dependent kinase 2 with two adenine derivative inhibitors reveals only one conserved hydrogen bond involving the NH of Leu<sup>83</sup> (26).

CKI7 may derive additional binding energy from its exocyclic chlorine at isoquinoline ring position 5, which is within hydrogen bonding distance of the hydroxyl group of Tyr<sup>59</sup>. This tyrosine is located in the inner surface of the nucleotide

binding cleft, comprises part of the P1 site, and is conserved in all CK1 isoforms identified to date (10).

**Interactions at the P3 Site.** The ethylamine sulfonamide chain of CKI7 makes unique contacts with a number of sidechains and water molecules in the P3 region (Figs. 1C and 2B). Part of this site is formed by the conserved decapeptide segment (Asp<sup>86</sup>-Leu-Leu-Gly-Pro-Ser-Leu-Glu-Asp-Leu<sup>95</sup>; loop L-5B and part of helix  $\alpha$ B) that connects the two lobes of CK1. The nitrogen N<sub>e</sub> (NH<sub>3</sub><sup>+</sup>) of the ethylamine sulfonamide chain, which is positively charged at physiological pH, interacts with the O<sub>δ2</sub> of Asp<sup>94</sup> as well as with Ser<sup>91</sup> and Asp<sup>94</sup> through two water molecules. A third water molecule bridges N<sub>β</sub> of CKI7 and the mainchain oxygen of Leu<sup>88</sup>. Although Leu<sup>88</sup>, Ser<sup>91</sup>, and Asp<sup>94</sup> are conserved in all known CK1 isoforms (10), the amino acid sequence diversity of the corresponding P3 sites among different protein kinases (19, 20) indicates that this site can be used to impart selectivity to potential inhibitors.

**Isoquinoline Ring-Flipping Model.** The availability of limited structure-activity relationship data for the isoquinoline sulfonamides suggests which of the interactions described above contribute to binding affinity and selectivity. In particular, comparison of CKI7 to *N*-(2-aminoethyl)-8-isoquinoline-sulfonamide (CKI6), which lacks the chlorine at position 5, and to H9, which contains the same substituents but at opposite positions on the isoquinoline ring, is instructive (Table 1). First, replacement of chlorine with hydrogen at isoquinoline ring position 5 (as in CKI6) results in an inhibitor that is 5-fold less potent than CKI7 against mammalian CK1. This suggests that the interaction between chlorine at position 5 and the hydroxyl group of Tyr<sup>59</sup> makes a significant contribution to CKI7 binding affinity. It must be noted, however, that CKI6 is less potent than CKI7 toward protein kinases that are unrelated to CK1 (11), and that do not contain a Tyr at the equivalent position. Thus, part of the difference in potency between CKI6 and CKI7 may result from other considerations, such as differences in their energies of desolvation (27, 28).

Second, switching the positions of the ethylamine sulfonamide chain to ring position 5 and the hydrogen to ring position 8 results in an inhibitor (H9, Table 1) that is only 2-fold less potent than CKI6 against mammalian CK1. This is surprising, as the structure of CK1–CKI7 predicts that the ethylamine sulfonamide in H9 should collide with the inner surface of the P1 site if the isoquinoline ring is oriented the same way as in CKI7. However, if the isoquinoline ring of H9 flips over, so that the sidechain attached to ring position 5 faces outside as in the CK1–CKI7 structure, substituents at position 5 can be tolerated. Assuming that the ring N2 atom maintains its interaction with the mainchain nitrogen of Leu<sup>88</sup> (Fig. 2C), such flipping could still maintain some of the interactions at the P3 site between the ethylamine sulfonamide chain and the protein, resulting in only a modest (2-fold) loss of potency.

Although this model suggests how isoquinoline sulfonamide selectivity among protein kinases is achieved, it is still unclear why differences in potency are observed within the CK1 family. For example, CKI7 inhibits fission yeast Cki1 with 4-fold

Fig. 1 (on opposite page). Structure of CK1–CKI7 complex. (A) Close up of the nucleotide binding cleft of CK1 showing the superimposition of the CKI7 and ATP (yellow). The GRASP (18) representation was computed at neutral pH and displayed at the level of the solvent-accessible surface. Charge distribution was color-coded with blue for positive, red for negative, and white for neutral. The CKI7 is represented by a stick model with white for carbon, dark blue for nitrogen, red for oxygen, green for sulfur, and magenta for chlorine. (B) Schematic illustration of the P1, P2, and P3 binding sites. The isoquinoline ring occupies the same position as the adenine ring of ATP (P1), whereas the ethylamine sulfonamide at ring position 8 (P3) extends in a different direction from the triphosphate (P2). The green cross in the lower right corner is a sulfate-binding site, where it may bind the phosphate moiety of phosphoprotein substrates (6). (C) Stereoview of a difference electron density map ( $F_o - F_c$ ,  $a_c$ ) contoured at 4 $\sigma$  above the mean. The CKI7 and three water molecules (W1, W2, and W3) were omitted in the structure factor calculation. Besides the charge and polar interactions, the isoquinoline ring of CKI7 is also surrounded by a number of hydrophobic amino acids: three leucines, three isoleucines, one valine, and one alanine. These van der Waals contacts (not shown) are the same as those observed for the adenine of ATP in CK1–MgATP complex (6). One CKI7 intramolecular hydrogen bond occurs between the nitrogen N<sub>e</sub> and the oxygen O<sub>α1</sub> of the sulfonate group (see Fig. 2B). (D) Structure-based amino acid sequence alignment of yeast Cki1<sup>16–298</sup> and mouse cAPK<sup>37–350</sup>. Identities are shown with vertical bars, whereas similarities are indicated by colons. Roman numerals mark the beginning of each of the 11 protein kinase subdomains (19). Secondary structure elements are only shown for Cki1<sup>16–298</sup>. Residues highlighted in Cki1<sup>16–298</sup> are either invariant (white against black) or similar (shaded) in all known isoforms of CK1. Residues highlighted in cAPK are those identified as being conserved in most protein kinases.

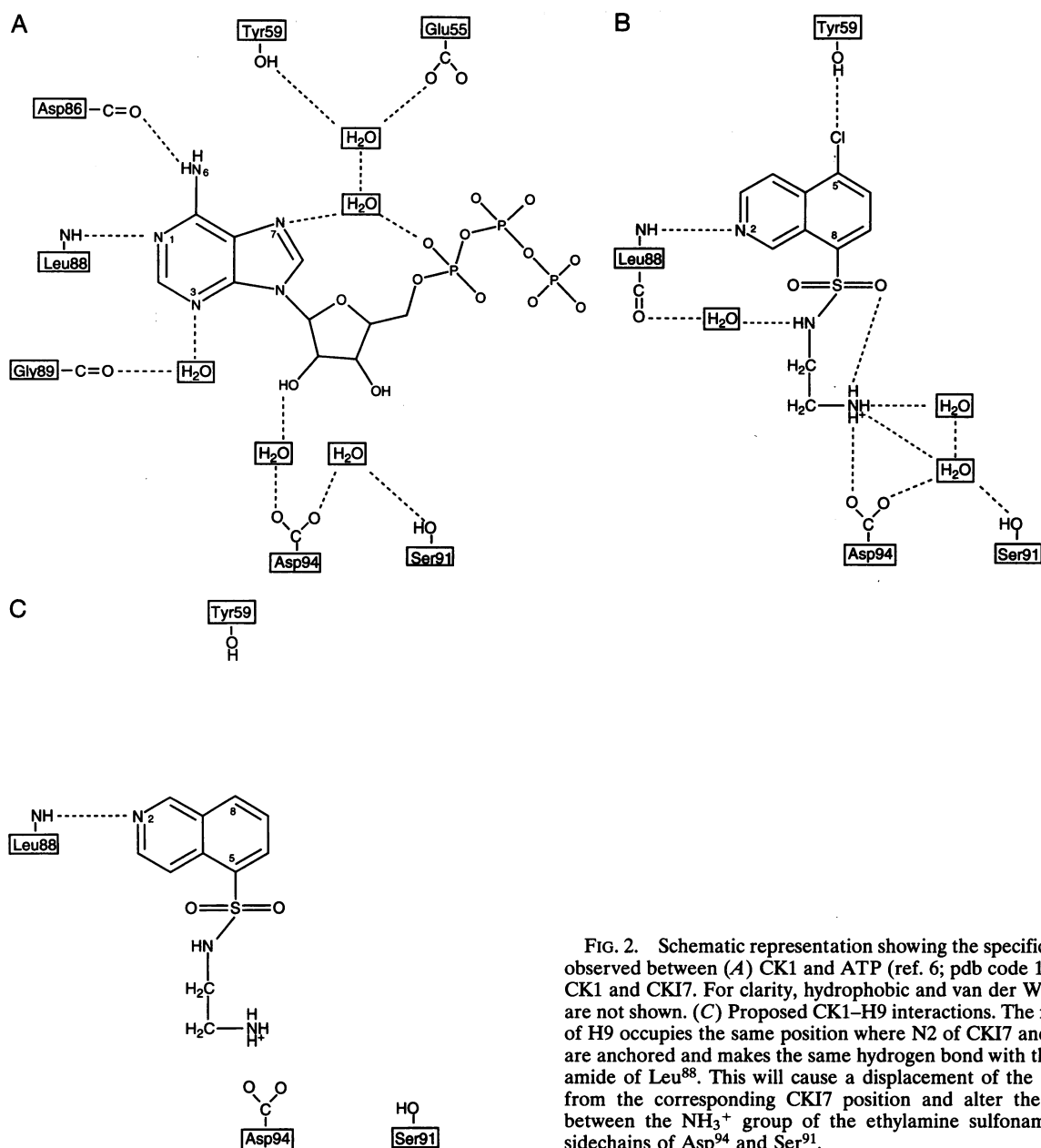


FIG. 2. Schematic representation showing the specific interactions observed between (A) CK1 and ATP (ref. 6; pdb code 1csn) and (B) CK1 and CKI7. For clarity, hydrophobic and van der Waals contacts are not shown. (C) Proposed CK1-H9 interactions. The ring N2 atom of H9 occupies the same position where N2 of CKI7 and N1 of ATP are anchored and makes the same hydrogen bond with the mainchain amide of Leu<sup>88</sup>. This will cause a displacement of the H9 molecule from the corresponding CKI7 position and alter the interactions between the NH<sub>3</sub><sup>+</sup> group of the ethylamine sulfonamide and the sidechains of Asp<sup>94</sup> and Ser<sup>91</sup>.

weaker potency than it inhibits mammalian CK1 (7, 10). It should be noted, however, that this lower potency for CKI7 is mirrored by a lower  $K_m$  for ATP (10), and so may result from differences in the conformation of the nucleotide-binding cleft that affects affinity but not selectivity. These in turn could arise from differences in primary structure (the catalytic domain of fission yeast and mammalian CK1 are approximately 55% identical in sequence), or from the influence of sequences outside the catalytic domain.

**Modelling of H9 with cAPK.** This ring-flipping model and the conservation of the hydrogen bond by the ring N2 atom also provide a possible structural explanation for the selectivity of H9 for cAPK relative to CK1 (ref. 7; see Table 1). In the cAPK structure, the region C terminal to the protein kinase catalytic domain, folds back toward the N-terminal lobe (21). One segment of this C-terminal region (Phe<sup>327</sup>-Asp<sup>328</sup>-Asp<sup>329</sup>-Tyr<sup>330</sup>; see Fig. 1D) forms part of the P3 site in cAPK, which may directly influence the inhibitor binding. To test the feasibility of this model, the interaction of H9 with cAPK was examined by molecular modelling methods (Fig. 3). When the N2 atom of an energy-minimized model of H9 is aligned to

hydrogen bond with the mainchain amide of Val<sup>123</sup> in the P1 site of cAPK the ethylamine sulfonamide chain of H9 molecule can be docked surprisingly well in the P3 site. In this model, the phenyl ring of Phe<sup>327</sup> interacts with the isoquinoline ring via the van der Waals contacts, whereas the hydroxyl group of Tyr<sup>330</sup>, the sidechain of Glu<sup>127</sup> and the mainchain oxygen of Leu<sup>49</sup> directly interact with the N<sub>e</sub> (NH<sub>3</sub><sup>+</sup>) of the ethylamine sulfonamide (Fig. 3).

The existence of other isoquinoline sulfonamides with very high affinity for cAPK, such as *N*-[2-(*p*-bromocinnamylamino)-ethyl]-5-isoquinolinesulfonamide (H89), which binds cAPK with a  $K_i$  of approximately 48 nM (ref. 9; see Table 1), suggest that additional interactions exist that increase ligand affinity and selectivity beyond those described above for H9. The long and bulky chain at ring position 5 of H89 could interact via a unique hydrogen bond between its bromine atom and the sidechain of Asp<sup>328</sup>, and by van der Waals contacts mediated by the aromatic ring of the benzene moiety.

**Summary.** The structure of the CK1-CKI7 complex provides a starting point for understanding the structural basis of the selectivity of the entire isoquinoline sulfonamide family of

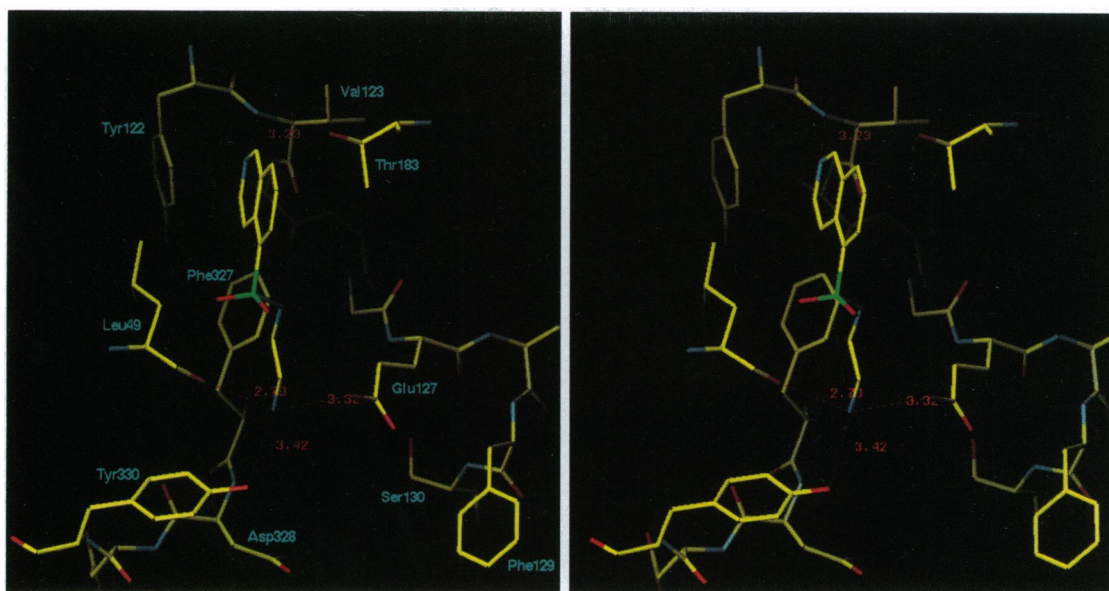


FIG. 3. Docking model for H9 binding in cAPK (ref. 21; pdb code 4cpk). The ring N2 atom makes a hydrogen bond with the mainchain nitrogen of Val<sup>123</sup>; the terminal NH<sub>3</sub><sup>+</sup> group of the ethylamine sulfonamide interacts with the sidechain of Glu<sup>127</sup> (the homologous of Ser<sup>91</sup> in CK1) and Tyr<sup>330</sup>, and the mainchain of Leu<sup>49</sup>.

inhibitors, and will facilitate the rational design of more effective protein kinase inhibitors. We have identified two sites, P1 and P3, as key to the selectivity of the isoquinoline sulfonamide class of ATP-competitive protein kinase inhibitors. Selectivity for protein kinases versus other enzymes is achieved by interactions in the P1 site, powered mostly by hydrophobic contacts and the hydrogen-bond forming nitrogen on isoquinoline ring. We propose that the hydrogen bond involving the ring N2 atom of the isoquinoline ring must be preserved in the P1 site, but that the ring can flip depending on the chemical substituents at positions 5 and 8. Selectivity for individual members of the protein kinase family is achieved primarily by interactions between these substituents and the P3 site, but also by specific interactions within the P1 site.

We thank T. Malone for assisting with protein purification and crystallization, R. M. Sweet for access to beamline X12-C of National Synchrotron Light Source (Brookhaven National Laboratory), and H. P. Nestler for help in modelling with MACROMODEL. We also thank N. Chester, A. Flint, J. Horton, G. Krafft, B. Shoichet, and X. Zhang for comments. The work was supported in part by National Institutes of Health Grants GM42816 and GM44806 to J.K. and the W. M. Keck Foundation to X.C. who holds the W.M. Keck Foundation endowed professorship in structural biology.

1. Tuazon, P. T. & Traugh, J. A. (1991) *Adv. Second Messenger Phosphoprotein Res.* **23**, 123–164.
2. Issinger, O.-G. (1993) *Pharmacol. Ther.* **59**, 1–30.
3. Cegielska, A. & Virshup, D. M. (1993) *Mol. Cell. Biol.* **13**, 1202–1211.
4. Milne, D. M., Palmer, R. H., Campbell, D. G. & Meek, D. W. (1992) *Oncogene* **7**, 1361–1369.
5. Hoekstra, M. F., Liskay, R. M., Ou, A. C., DeMaggio, A. J., Burbee, D. G. & Heffron, F. (1991) *Science* **253**, 1031–1034.
6. Xu, R.-M., Carmel, G., Sweet, R. M., Kuret, J. & Cheng, X. (1995) *EMBO J.* **14**, 1015–1023.
7. Chijiwa, T., Hagiwara, M. & Hidaka, H. (1989) *J. Biol. Chem.* **264**, 4924–4927.
8. Hagiwara, M., Inagaki, M. & Hidaka, H. (1987) *Mol. Pharmacol.* **31**, 523–528.
9. Chijiwa, T., Mishima, A., Hagiwara, M., Sano, M., Hayashi, K., Inoue, T., Naito, K., Toshioka, T. & Hidaka, H. (1990) *J. Biol. Chem.* **265**, 5267–5272.

10. Wang, P.-C., Vancura, A., Desai, A., Carmel, G. & Kuret, J. (1994) *J. Biol. Chem.* **269**, 12014–12023.
11. Casnellie, J. E. (1991) *Adv. Pharmacol.* **22**, 167–205.
12. Hidaka, H. & Kobayashi, R. (1993) in *Protein Phosphorylation: A Practical Approach*, ed. Hardie, D. G. (Oxford University Press, New York), pp. 87–107.
13. Carmel, G., Leichus, B., Cheng, X., Patterson, S. O., Mirza, U., Chait, B. T. & Kuret, J. (1994) *J. Biol. Chem.* **269**, 7304–7309.
14. Otwinowski, Z. (1993) in *Data Collection and Processing*, eds. Sawyer, L., Issacs, N. & Bailey, S. (SERC Daresbury Laboratory, Warrington, U.K.), pp. 56–62.
15. Brünger, A. T., Karplus, M. & Petsko, G. A. (1989) *Acta Crystallogr. A* **45**, 50–61.
16. Jones, T. A., Zou, J. Y., Cowan, S. W. & Kjeldgaard, M. (1991) *Acta Crystallogr. A* **47**, 110–119.
17. Mohamadi, F., Richards, N. G. J., Guida, W. C., Liskamp, R. M. J., Lipton, M. A., Caufield, C. E., Chang, G., Hendrickson, T. F. & Still, W. C. (1990) *J. Comput. Chem.* **11**, 440–467.
18. Nicholls, A., Sharp, K. A. & Honig, B. (1991) *Proteins Struct. Funct. Genet.* **11**, 281–296.
19. Hanks, S. K., Quinn, A. M. & Hunter, T. (1988) *Science* **241**, 42–52.
20. Hanks, S. K. & Quinn, A. M. (1991) *Methods Enzymol.* **200**, 38–62.
21. Zheng, J., Knighton, D. R., Ten Eyck, L. F., Karlsson, R., Xuong, N.-H., Taylor, S. S. & Sowadski, J. M. (1993) *Biochemistry* **32**, 2154–2161.
22. De Bondt, H. L., Rosenblatt, J., Jancarik, J., Jones, H. D., Morgan, D. O. & Kim, S.-H. (1993) *Nature (London)* **363**, 595–602.
23. Zhang, F., Strand, A., Robbins, D., Cobb, M. H. & Goldsmith, E. J. (1994) *Nature (London)* **367**, 704–711.
24. Owen, D. J., Noble, M. E. M., Garman, E. F., Papageorgiou, A. C. & Johnson, L. N. (1995) *Structure* **3**, 467–482.
25. Hidaka, H., Inagaki, M., Kawamoto, S. & Sasaki, Y. (1984) *Biochemistry* **23**, 5036–5041.
26. Schulze-Gahman, U., Brandsen, J., Jones, H. D., Morgan, D. O., Meijer, L., Vesely, J. & Kim, S.-H. (1995) *Proteins Struct. Funct. Genet.* **22**, 378–391.
27. Warshel, A., Aqvist, J. & Creighton, S. (1989) *Proc. Natl. Acad. Sci. USA* **86**, 5820–5824.
28. Warncke, K. & Dutton, P. L. (1993) *Proc. Natl. Acad. Sci. USA* **90**, 2920–2924.